Int. J. Heat Mass Transfer. Vol. 7, pp. 863–874. Pergamon Press 1964. Printed in Great Britain

LAMINAR FREE CONVECTION NEAR THE LOWER STAGNATION POINT ON AN ISOTHERMAL CURVED SURFACE

G. POOTS
Department of Theoretical Mechanics, University of Bristol

(*Received* 15 *February* 1964)

Abstract—This paper deals with some aspects of the three dimensional laminar free convection boundary layer near the stagnation point on a general curved isothermal surface, which is maintained at a temperature above the ambient temperature of the fluid. Thus the stagnation point is defined as the lowest (elliptic) point on the surface and such that the tangent plane at this point is horizontal. Boundary-layer equations are formulated and it is shown that the flow at the stagnation point depends on the ratio of the two principal radii of curvature at this point, the Prandtl number and the Grashof number. These equations are solved numerically for Prandtl number 0·72 and for various values of the ratio of the two principal radii of curvature.

For the stagnation point flow there are two limiting cases, namely the flow at the lower stagnation line on a uniform horizontal cylinder and that at the lower stagnation point on a sphere. The numerical solutions for the sphere and cylinder are then used to develop an approximate method of solution for the stagnation point on a general curved surface; good agreement with the precise numerical solutions was obtained.

NOMENCLATURE

A, B, C,	scalars;
$\mathbf{a}, \mathbf{a}_2$,	unit vectors on S;
a, b,	minor and major axis of an ellipsoid;
$A_i(\alpha)$,	$i = 1, 2, 3$, mixing parameters;
E, F, G,	fundamental magnitudes of the first order;
$\mathbf{F}$,	vector gravitational body force;
f, g, h, F, G, H,	velocity and thermal profiles;
$Gr = \beta g (T_0 - T_\infty) R_2^3/\nu^2$,	the Grashof number;
$\mathbf{g} = g\mathbf{n}_0$,	acceleration due to gravity;
$\mathbf{i}, \mathbf{j}, \mathbf{k}$,	unit vectors in the x, y, z directions;
J_σ	first curvature of the surface σ;
k,	the thermal diffusivity;
L, M, N,	fundamental magnitudes of the second order;
Nu,	Nusselt number;
$\mathbf{n}$,	unit normal to the surface S;
p,	the pressure;
Pr,	the Prandtl number;
$\mathbf{r} = \mathbf{r}(x_1, x_2)$,	position vector of a point on S;
$\mathbf{R}$,	position vector of a point in space;
R_1, R_2,	principal radii of curvature at O;
T,	temperature;
$\mathbf{u} = \mathbf{a}_1 u_1 + \mathbf{a}_2 u_2$,	velocity vector parallel to S;
$\mathbf{v} = \mathbf{u} + \mathbf{n}\, v_3$,	velocity vector in space;
v_1, v_2, v_3,	velocity vectors in the $\mathbf{a}_1$, $\mathbf{a}_2$ and $\mathbf{n}$ directions;
V_1, V_2, V_3,	dimensionless velocity components;
x, y, z,	Cartesian co-ordinates;
x_1, x_2, x_3,	curvilinear co-ordinates;
X_1, X_2, X_3,	dimensionless curvilinear co-ordinates.

Greek symbols

α,	square root of the ratio of the principal radii;
β,	coefficient of cubical expansion;
ν,	kinematic viscosity;

ϵ, angle between velocity or shear stress vectors;
τ_1, τ_2, components of shear stress;
Θ, dimensionless temperature;
ρ, density;
$\eta = Gr^{1/4}X_3$, dimensionless independent variable.

Subscripts
∞, ambient condition;
o, stagnation point condition;
D, dynamic condition;
S, surface of body;
σ, surface in space parallel to S.

1. INTRODUCTION

MUCH theoretical and experimental work has been done on the free convection boundary layer (see Ede [1]). The theoretical investigations deal mainly with two dimensional boundary layers on isothermal or non-isothermal surfaces, where similar solutions or Blasius-type expansions of the boundary-layer equations can be found. Several investigations of axisymmetric free convection flows have been reported. Merk and Prins [2] derived the general relations for the existence of similar solutions to axisymmetric shapes such as the cone; further solutions to the axisymmetric flow problem have been obtained by Braun *et al.* [3] and Hering and Grosh [4].

The purpose of this investigation is to present some information on the three dimensional free convection boundary layer near the lower stagnation point on an isothermal curved surface. The surface is maintained at a temperature above the ambient temperature of the fluid and it is assumed that the stagnation point is the lowest minimum point of the surface and such that the tangent plane at this point is horizontal. Following reference [5a] the three dimensional boundary-layer equations, which govern the free convection flow near the stagnation point, are formulated. If the parametric lines of the curvilinear co-ordinates on the surface are chosen to be lines of curvature, a similar solution of the boundary-layer equations can be found. This solution depends on the Prandtl number, Grashof number and geometrically on the ratio of the two principal radii of curvature of the surface at the stagnation point. Thus geometrical properties of the surface appear explicitly in the equations as distinct from the corresponding equations for forced flow as discussed by Howarth [6]. There, on examination of the boundary-layer equations, the forced flow is seen to depend on the nature of the external irrotational flow at the edge of the boundary layer. In fact Howarth's solution is an exact solution of the full equations of viscous motion in Cartesian co-ordinates.

To examine the effect of different radii of curvature on the local flow and heat-transfer characteristics at the stagnation point, the similar solution of the boundary-layer equations is evaluated numerically for Prandtl number 0·72 and for various ratios of the two principal radii of curvature. There are two limiting cases, namely the flow near the lower stagnation line on a uniform horizontal cylinder and that near the lower stagnation point on a sphere. Using the numerical solutions for these limiting cases, suitable velocity and thermal profiles are chosen which contain unknown parameters. These parameters are then found using the Pohlhausen method [5b] and so giving approximate information for all ratios of the two principal radii of curvature. These approximate results for the flow and heat-transfer characteristics are found to be in good agreement with the precise numerical solutions.

2. DERIVATION OF THE BOUNDARY-LAYER EQUATIONS

Laminar free convection on a general curved isothermal surface is governed by the following equations:

$$(\mathbf{v}.\nabla)\mathbf{v} = \nu\nabla^2\mathbf{v} - \frac{1}{\rho}\nabla p + \frac{1}{\rho}\mathbf{F}, \qquad (1)$$

$$\text{div}\,\mathbf{v} = 0 \qquad (2)$$

and

$$(\mathbf{v}.\nabla)T = k\,\text{div}\,\nabla T, \qquad (3)$$

where ∇ denotes the gradient operator in three dimensional space. In equations (1) to (3) it has been assumed that all physical properties of the fluid are independent of the temperature, and that allowance is made for variations in the density only in the calculation of the body force **F**. Moreover, in equation (3) the viscous dissipation and work done against compression have been omitted.

The gravitational body force **F** per unit volume of fluid is

$$\mathbf{F} = \rho \mathbf{g}, \tag{4}$$

and the appropriate equation of state is

$$\frac{\rho - \rho_\infty}{\rho_\infty} = -\beta(T - T_\infty), \tag{5}$$

where β is the coefficient of thermal expansion.

Following reference [5a] the surface of the body S is defined by the equation

$$\mathbf{r} = \mathbf{r}(x_1, x_2), \tag{6}$$

where x_1 and x_2 are orthogonal curvilinear co-ordinates on S. Let $P'(x_1, x_2)$, a point on S, be the foot of a perpendicular drawn from a point P in space, then the vector position of P is

$$\mathbf{R} = \mathbf{r}(x_1, x_2) + x_3\, \mathbf{n}(x_1, x_2), \tag{7}$$

where $\mathbf{n}$ is the unit normal to S at P' and x_3 is the distance PP'. The co-ordinate system x_1, x_2, x_3 is now triply orthogonal on S but not necessarily elsewhere. The boundary-layer equations are now derived from the equations (1) to (3) in terms of this system of co-ordinates.

The gradient operator ∇_s for the surface S is (see Weatherburn [7])

$$\nabla_s = \frac{\mathbf{a}_1}{h_1}\frac{\partial}{\partial x_1} + \frac{\mathbf{a}_2}{h_2}\frac{\partial}{\partial x_2} \tag{8}$$

where

$$h_1 = \left|\frac{\partial \mathbf{r}}{\partial x_1}\right|,\ h_2 = \left|\frac{\partial \mathbf{r}}{\partial x_2}\right|,\ \mathbf{a}_1 h_1 = \frac{\partial \mathbf{r}}{\partial x_1}$$
$$\text{and } \mathbf{a}_2 h_2 = \frac{\partial \mathbf{r}}{\partial x_2}; \tag{9}$$

$\mathbf{a}_1$, $\mathbf{a}_2$ are unit vectors on S which are tangential to the two parametric curves through $P'(x_1, x_2)$. As derived in [5a] the gradient operator for space is

$$\nabla = \nabla_\sigma + \mathbf{n}\frac{\partial}{\partial x_3}$$
$$= \nabla_s + \mathbf{n}\frac{\partial}{\partial x_3} + 0(x_3); \tag{10}$$

and if

$$H = \mathbf{a}_1 H_1 + \mathbf{a}_2 H_2 + \mathbf{n} H_3, \tag{11}$$

then

$$\operatorname{div} \mathbf{H} = \frac{1}{h_1 h_2}\left\{\frac{\partial}{\partial x_1}(h_2 H_1) + \frac{\partial}{\partial x_2}(h_1 H_2)\right\} + \frac{\partial H_3}{\partial x_3} - J_\sigma H_3. \tag{12}$$

Here the suffix σ denotes a surface in space parallel to S, J_σ is the first curvature of the surface σ, and **H** is any representative vector.

Consider now a particular surface S such that there is a minimum point on the surface at O, which is chosen to be the origin of the orthogonal co-ordinates x_1, and x_2; let the unit normal $\mathbf{n}_0$ to the surface at this point be in the vertical downward direction. If the surface is maintained at a temperature $T_s > T_\infty$ then steady free convection flow will originate from this point provided it is the lowest point on the isothermal curved surface. In geometrical terms the lower stagnation point must be the *min.* elliptic point of the surface. Note that if $T_s > T_\infty$ the upper stagnation point must be the *max.* point of the surface.

Suppose that thermal and viscous effects are confined to a thin boundary layer next to S, and for convenience put

$$\mathbf{v} = \mathbf{u} + \mathbf{n}v_3 = \mathbf{a}_1 v_1 + \mathbf{a}_2 v_2 + \mathbf{n} v_3. \tag{13}$$

Thus x_3 and v_3 are small and derivatives with respect to x_3 are large compared with those with respect to x_1 and x_2. From [5a] the momentum equation (1) becomes

$$\left(\mathbf{u}.\nabla_s + v_3\frac{\partial}{\partial x_3}\right)(\mathbf{u} + \mathbf{n}v_3) = \nu\frac{\partial^2}{\partial x_3^2}(\mathbf{u} + \mathbf{n}v_3) - \frac{1}{\rho}\left(\nabla_s p + \mathbf{n}\frac{\partial p}{\partial x_3}\right) - \frac{1}{\rho}\mathbf{F}, \tag{14}$$

where

$$\mathbf{F} = \rho g\, \mathbf{n}_0. \tag{15}$$

The appropriate boundary-layer equations for v_1, v_2 and v_3 can now be given once **F** has been resolved in the directions $\mathbf{a}_1$, $\mathbf{a}_2$, and $\mathbf{n}$, i.e. in directions parallel and normal to the surface at the point (x_1, x_2, x_3). Let

$$\mathbf{n}_0 = A\,\mathbf{a}_1 + B\,\mathbf{a}_2 + C\mathbf{n}, \tag{16}$$

where A, B and C are scalars defined by

$$A = \mathbf{n}_0 \cdot \mathbf{a}_1,\ B = \mathbf{n}_0 \cdot \mathbf{a}_2,\ C = \mathbf{n}_0 \cdot \mathbf{n}. \tag{17}$$

These are evaluated by expanding $\mathbf{a}_1$, $\mathbf{a}_2$ and $\mathbf{n}$ in the form of a Taylor series about the stagnation point $x_1 = x_2 = 0$; thus if x_1 and x_2 are small

$$\mathbf{a}_1 = (\mathbf{a}_1)_0 + x_1\left(\frac{\partial \mathbf{a}_1}{\partial x_1}\right)_0 + x_2\left(\frac{\partial \mathbf{a}_1}{\partial x_2}\right)_0 + \dots,$$

$$\mathbf{a}_2 = (\mathbf{a}_2)_0 + x_1\left(\frac{\partial \mathbf{a}_2}{\partial x_1}\right)_0 + x_2\left(\frac{\partial \mathbf{a}_2}{\partial x_2}\right)_0 + \dots, \tag{18}$$

and

$$\mathbf{n} = (\mathbf{n}_0) + x_1\left(\frac{\partial \mathbf{n}}{\partial x_1}\right)_0 + x_2\left(\frac{\partial \mathbf{n}}{\partial x_2}\right)_0 + \dots.$$

Expressions for the above derivatives are given by Weatherburn [7] as follows:

$$\left.\begin{aligned}
\frac{\partial \mathbf{a}_1}{\partial x_1} &= \frac{L}{h_1}\mathbf{n} - \frac{1}{h_2}\frac{\partial h_1}{\partial x_2}\mathbf{a}_2,\\
\frac{\partial \mathbf{a}_1}{\partial x_2} &= \frac{M}{h_1}\mathbf{n} + \frac{1}{h_1}\frac{\partial h_1}{\partial x_1}\mathbf{a}_2,\\
\frac{\partial \mathbf{a}_2}{\partial x_1} &= \frac{M}{h_2}\mathbf{n} + \frac{1}{h_2}\frac{\partial h_1}{\partial x_2}\mathbf{a}_1,\\
\frac{\partial \mathbf{a}_2}{\partial x_2} &= \frac{N}{h_2}\mathbf{n} - \frac{1}{h_1}\frac{\partial h_2}{\partial x_1}\mathbf{a}_1.
\end{aligned}\right\} \tag{19}$$

The quantities L, M, N are known as fundamental magnitudes of the second order and are related to the quantities E, F, G, known as fundamental magnitudes of the first order by the relations:

$$\left.\begin{aligned}
E &= \mathbf{r}_1 \cdot \mathbf{r}_1 = h_1^2,\\
F &= \mathbf{r}_1 \cdot \mathbf{r}_2,\\
G &= \mathbf{r}_2 \cdot \mathbf{r}_2 = h_2^2,\\
L &= [\mathbf{r}_1\, \mathbf{r}_2\, \mathbf{r}_{11}]/(EG - F^2)^{1/2},\\
M &= [\mathbf{r}_1\, \mathbf{r}_2\, \mathbf{r}_{12}]/(EG - F^2)^{1/2},\\
N &= [\mathbf{r}_1\, \mathbf{r}_2\, \mathbf{r}_{22}]/(EG - F^2)^{1/2}.
\end{aligned}\right\} \tag{20}$$

Here the suffix 1 or 2 on $\mathbf{r}$ denotes partial differentiation with respect to x_1 or x_2, i.e.

$$\mathbf{r}_1 = \frac{\partial \mathbf{r}}{\partial x_1},\ \mathbf{r}_{12} = \frac{\partial^2 \mathbf{r}}{\partial x_1\, \partial x_2};$$

in the usual notation $[\mathbf{r}_1\, \mathbf{r}_2\, \mathbf{r}_{12}]$ denotes a triple scalar product. On using expressions (17), (18) and (19), there results:

$$\left.\begin{aligned}
A &= \mathbf{n}_0 \cdot (\mathbf{a}_1)_0 + x_1\, \mathbf{n}_0 \cdot \left(\frac{\partial \mathbf{a}_1}{\partial x_1}\right)_0\\
&\quad + x_2\, \mathbf{n}_0 \cdot \left(\frac{\partial \mathbf{a}_1}{\partial x_2}\right)_0 + \dots\\
&= x_1\, \mathbf{n}_0 \cdot \left(\frac{L}{h_1}\mathbf{n} - \frac{1}{h_2}\frac{\partial h_1}{\partial x_2}\mathbf{a}_2\right)_0 + \dots\\
&\quad + x_2\, \mathbf{n}_0 \cdot \left(\frac{M}{h_1}\mathbf{n} + \frac{1}{h_1}\frac{\partial h_1}{\partial x_2}\mathbf{a}_2\right)_0 + \dots\\
&= \left(\frac{L}{h_1}\right)_0 x_1 + \left(\frac{M}{h_1}\right)_0 x_2 + \dots;
\end{aligned}\right\} \tag{21}$$

in a similar fashion it follows that

$$B = \left(\frac{M}{h_2}\right)_0 x_1 + \left(\frac{N}{h_2}\right)_0 x_2 + \dots, \tag{22}$$

and finally since $\mathbf{n} = \mathbf{a}_1 \times \mathbf{a}_2$ it can be shown that

$$C = 1 + \dots. \tag{23}$$

Correct to terms of order x_1 and x_2 the components of the body force $\mathbf{F}$ in the directions of the unit vectors $\mathbf{a}_1$, $\mathbf{a}_2$ and $\mathbf{n}$, at a point x_1 and x_2, are:

$$\mathbf{F} = \rho g \left[\left(\frac{L}{h_1}\right)_0 x_1 + \left(\frac{M}{h_1}\right)_0 x_2,\ \left(\frac{M}{h_2}\right)_0 x_1 + \left(\frac{N}{h_2}\right)_0 x_2,\ 1\right]. \tag{24}$$

Consider the $\mathbf{n}$-component of equation (14); the principal terms give:

$$\rho\left(\frac{L}{h_1^2}v_1^2 + \frac{2M}{h_1 h_2}v_1 v_2 + \frac{N}{h_2^2}v_2^2\right) = -\frac{\partial p}{\partial x_3} - \rho g. \tag{25}$$

Let

$$p = p_D - \rho_\infty g\, x_3, \tag{26}$$

where p_D is the 'dynamic' pressure and $\rho_\infty g\, x_3$ is the hydrostatic pressure in the absence of heating. It follows from (25) that the variation in p_D across the boundary layer is small, and it is assumed that p_D is independent of x_3. The $\mathbf{a}_1$ and $\mathbf{a}_2$-components of the momentum equation (14) now yield:

$$\left.\begin{aligned}\rho\left(\frac{v_1}{h_1}\frac{\partial v_1}{\partial x_1}+\frac{v_2}{h_2}\frac{\partial v_1}{\partial x_2}+v_3\frac{\partial v_1}{\partial x_3}+\frac{v_1v_2}{h_1h_2}\frac{\partial h_1}{\partial x_2}\right.\\ \left.-\frac{v_2^2}{h_1h_2}\frac{\partial h_2}{\partial x_1}\right)=\rho\nu\frac{\partial^2 v_1}{\partial x_3^2}-\frac{1}{h_1}\frac{\partial p_D}{\partial x_1}\\ -\rho g\left\{\left(\frac{L}{h_1}\right)_0 x_1+\left(\frac{M}{h_1}\right)_0 x_2\right\},\end{aligned}\right\} \quad (27)$$

and

$$\left.\begin{aligned}\rho\left(\frac{v_1}{h_1}\frac{\partial v_2}{\partial x_1}+\frac{v_2}{h_2}\frac{\partial v_2}{\partial x_2}+v_3\frac{\partial v_2}{\partial x_3}-\frac{v_1^2}{h_1h_2}\frac{\partial h_1}{\partial x_2}\right.\\ \left.+\frac{v_1v_2}{h_1h_2}\frac{\partial h_2}{\partial x_1}\right)=\rho\nu\frac{\partial^2 v_2}{\partial x_3^2}-\frac{1}{h_2}\frac{\partial p_D}{\partial x_2}\\ -\rho g\left\{\left(\frac{M}{h_2}\right)x_1+\left(\frac{N}{h_2}\right)_0 x_2\right\},\end{aligned}\right\} \quad (28)$$

respectively. As v_1 and v_2 tend to zero at the edge of the boundary layer, equations (27) and (28) imply:

$$\frac{1}{h_2}\frac{\partial p_D}{\partial x_1}=-\rho_\infty g\left\{\left(\frac{L}{h_1}\right)_0 x_1+\left(\frac{M}{h_1}\right)_0 x_2\right\}$$

and

$$\frac{1}{h_2}\frac{\partial p_D}{\partial x_2}=-\rho_\infty g\left\{\left(\frac{M}{h_2}\right)_0 x_1+\left(\frac{N}{h_2}\right)_0 x_2\right\}. \quad (29)$$

Inserting expressions (29) in (27) and (28) and using (5) the boundary-layer equations for the flow in the vicinity of the stagnation point are:

$$\left.\begin{aligned}\frac{v_1}{h_1}\frac{\partial v_1}{\partial x_1}+\frac{v_2}{h_2}\frac{\partial v_1}{\partial x_2}+v_3\frac{\partial v_1}{\partial x_3}+\frac{v_1v_2}{h_1h_2}\frac{\partial h_1}{\partial x_2}\\ -\frac{v_2^2}{h_1h_2}\frac{\partial h_2}{\partial x_1}=\nu\frac{\partial^2 v_1}{\partial x_3^2}+g\beta(T-T_\infty)\\ \times\left\{\left(\frac{L}{h_1}\right)_0 x_1+\left(\frac{M}{h_1}\right)_0 x_2\right\},\end{aligned}\right\} \quad (30)$$

and

$$\left.\begin{aligned}\frac{v_1}{h_1}\frac{\partial v_2}{\partial x_1}+\frac{v_2}{h_2}\frac{\partial v_2}{\partial x_2}+v_3\frac{\partial v_2}{\partial x_3}-\frac{v_1^2}{h_1h_2}\frac{\partial h_1}{\partial x_2}\\ +\frac{v_1v_2}{h_1h_2}\frac{\partial h_2}{\partial x_1}=\nu\frac{\partial^2 v_2}{\partial x_3^2}+g\beta(T-T_\infty)\\ \times\left\{\left(\frac{M}{h_2}\right)_0 x_1+\left(\frac{N}{h_2}\right)_0 x_2\right\}.\end{aligned}\right\} \quad (31)$$

To within the same order of approximation (see [5a]) the equation of continuity is

$$\frac{1}{h_1h_2}\left\{\frac{\partial}{\partial x_1}(h_2v_1)+\frac{\partial}{\partial x_2}(h_1v_2)\right\}+\frac{\partial v_3}{\partial x_3}=0, \quad (32)$$

and the thermal energy equation (3) becomes:

$$\frac{v_1}{h_1}\frac{\partial T}{\partial x_1}+\frac{v_2}{h_2}\frac{\partial T}{\partial x_2}+v_3\frac{\partial T}{\partial x_3}=k\frac{\partial^2 T}{\partial x_3{}^2}. \quad (33)$$

Finally the boundary conditions are:

$$v_1=v_2=v_3=0,\ T=T_0 \quad \text{when} \quad x_3=0,$$

and

$$v_1 -> 0,\ v_2 -> 0,\ T -> T_\infty \text{ as } x_3 -> \infty. \quad (34)$$

In the above equations all physical properties are to be evaluated at the ambient condition.

These equations are complicated as they involve quantities related to the geometry of the surface such as the fundamental magnitudes of the first and second order. As the values of these quantities are dependent on the choice of the coordinate system it does not appear possible to infer any general information from the above equations in their present form. This difficulty can be removed if the parametric lines $x_1 =$ const. and $x_2 =$ const. are taken to be lines of curvature on the surface. The necessary and sufficient conditions for the parametric lines to be lines of curvature are

$$F=M=0. \quad (35)$$

Moreover, since the surface is regular at the stagnation point, it is permissible to expand h_1 and h_2 as follows:

$$\left.\begin{aligned}h_1&=\\ &(h_1)_0+x_1\left(\frac{\partial h_1}{\partial x_1}\right)_0+x_2\left(\frac{\partial h_1}{\partial x_2}\right)_0+\ldots,\\ h_2&=\\ &(h_2)_0+x_1\left(\frac{\partial h_2}{\partial x_1}\right)_0+x_2\left(\frac{\partial h_2}{\partial x_2}\right)_0+\ldots.\end{aligned}\right\} \quad (36)$$

On substitution of (35) into equations (30) and (31) it follows that v_1 and v_2 are of the same order as the buoyancy forces, i.e. of $0(x_1)$ or $0(x_2)$. Using this fact, and the expansions given in (36), the principal terms of the boundary-layer equations (30) to (33) are:

$$\frac{v_1}{h_1}\frac{\partial v_1}{\partial x_1} + \frac{v_2}{h_2}\frac{\partial v_1}{\partial x_2} + v_3\frac{\partial v_1}{\partial x_3} = \nu\frac{\partial^2 v_1}{\partial x_3^2} + g\beta\,(T - T_\infty)\left(\frac{L}{E}\right) h_1\, x_1, \quad (37)$$

$$\frac{v_1}{h_1}\frac{\partial v_2}{\partial x_1} + \frac{v_2}{h_2}\frac{\partial v_2}{\partial x_2} + v_3\frac{\partial v_2}{\partial x_3} = \nu\frac{\partial^2 v_2}{\partial x_3^2} + g\beta\,(T - T_\infty)\left(\frac{N}{G}\right) h_2\, x_2, \quad (38)$$

$$\frac{1}{h_1}\frac{\partial v_1}{\partial x_1} + \frac{1}{h_2}\frac{\partial v_2}{\partial x_2} + \frac{\partial v_3}{\partial x_3} = 0, \quad (39)$$

and

$$\frac{v_1}{h_1}\frac{\partial T}{\partial x_1} + \frac{v_2}{h_2}\frac{\partial T}{\partial x_2} + v_3\frac{\partial T}{\partial x_3} = k\frac{\partial^2 T}{\partial x_3^2}. \quad (40)$$

Here the suffix 0 on the quantities h_1, h_2, E, G, L and N has been omitted. Now the principal radii of curvature at any point on the surface are expressed in terms of the first and second fundamental magnitudes by the equation:

$$(LN - M^2)\, R^2 + (2MF - LG - NE)\, R + (EG - F^2) = 0; \quad (41)$$

due to the co-ordinate restriction (35) it is clear that E/L and G/N are the two principal radii of curvature at the stagnation point.

For convenience, let

$$R_1 = \frac{E}{L} \text{ and } R_2 = \frac{G}{N}, \quad (42)$$

and such that $R_2 \leqslant R_1$. The boundary-layer equations are now made non-dimensional on taking R_2, ν/R_2 and $(T_0 - T_\infty)$ to be representative length, velocity and temperature scales respectively. New dependent and independent variables are chosen as follows:

$$h_1\, x_1 = R_2\, X_1, \quad h_2\, x_2 = R_2\, X_2, \quad x_2 = R_2\, X_3,$$

$$v_1 = \sqrt{\left(\frac{R_2}{R_1}\right)}\frac{\nu}{R_2} V_1, \quad v_2 = \frac{\nu}{R_2} V_2, \quad v_3 = \frac{\nu}{R_2} V_3, \quad (43)$$

and

$$\Theta = \frac{T - T_\infty}{T_0 - T_\infty}.$$

Equations (37) to (40) become:

$$a\, V_1\frac{\partial V_1}{\partial X_1} + V_2\frac{\partial V_1}{\partial X_2} + V_3\frac{\partial V_1}{\partial X_3} = \frac{\partial^2 V_1}{\partial X_3^2} + a\, G X_1\, \Theta, \quad (44)$$

$$a\, V_1\frac{\partial V_2}{\partial X_1} + V_2\frac{\partial V_2}{\partial X_2} + V_3\frac{\partial V_2}{\partial X_3} = \frac{\partial^2 V_2}{\partial X_3^2} + G X_2\, \Theta, \quad (45)$$

$$a\frac{\partial V_1}{\partial X_1} + \frac{\partial V_2}{\partial X_2} + \frac{\partial V_3}{\partial X_3} = 0, \quad (46)$$

and

$$Pr\left(a\, V_1\frac{\partial \Theta}{\partial X_1} + V_2\frac{\partial \Theta}{\partial X_2} + V_3\frac{\partial \Theta}{\partial X_3}\right) = \frac{\partial^2 \Theta}{\partial X_3^2}; \quad (47)$$

the boundary conditions are:

$$\left.\begin{aligned} &V_1 = V_2 = V_3 = 0, \quad \Theta = 1 \text{ when } x_3 = 0, \\ &V_1 \to 0, \quad V_2 \to 0, \quad \Theta \to 0 \text{ as } X_3 \to \infty. \end{aligned}\right\} \quad (48)$$

Here $a = \sqrt{(R_2/R_1)}$, $Pr = \nu/k$ is the Prandtl number and $Gr = \beta g\,(T_0 - T_\infty)\, R_2^3/\nu^2$ is the Grashof number.

3. SIMILAR SOLUTION OF THE BOUNDARY-LAYER EQUATIONS

In terms of the variable

$$\eta = Gr^{1/4}\, X_3, \quad (49)$$

the similar solution of the non-dimensional boundary-layer equations (44) to (47), subject to the boundary conditions (48), is of the form:

$$\left.\begin{aligned} &V_1 = Gr^{1/4}\, X_1 f', \quad V_2 = Gr^{1/4}\, X_2\, g', \\ &V_3 = -(g + af) \\ &\text{and} \quad \Theta = h, \end{aligned}\right\} \quad (50)$$

where f, g and h are functions of η only, and the dash denotes differentiation with respect to η. These functions satisfy the following non-linear ordinary differential equations:

$$f''' + (g + af)\, f'' - a\,(f')^2 + ah = 0, \quad (51)$$

$$g''' + (g + af)\, g'' - (g')^2 + h = 0, \qquad (52)$$

and

$$h'' + Pr\,(g + af)\, h' = 0, \qquad (53)$$

subject to the boundary conditions:

$$\left.\begin{array}{l} f(0) = f'(0) = g(0) = g'(0),\, h(0) = 1, \\ f'(\infty) = g'(\infty) = h(\infty) = 0. \end{array}\right\} \qquad (54)$$

Equations (51) to (54) define an eighth order boundary value problem. They contain the parameters: Pr the Prandtl number, and a the square root of the ratio of the two principal radii of curvature at the stagnation point. There are two special cases:

(i) $a = 0$, which corresponds to the two-dimensional free convection flow near the stagnation line on a uniform horizontal cylinder. In this case $f \equiv 0$, and

$$g''' + gg'' - (g')^2 + h = 0, \qquad (54)$$

$$h'' + Pr\, gh' = 0, \qquad (55)$$

where

$$g(0) = g'(0) = 0,\, h(0) = 1,$$
$$g(\infty) = h(\infty) = 0. \qquad (56)$$

These equations have previously been derived by Prins and Merk [2]. In a discussion of Hermann's approximate solution [8] for the free convection flow around a heated horizontal cylinder, Chen [9] also notes that a similar solution can be found for the lower stagnation line.

(ii) $a = 1$, which corresponds to the flow near the lower stagnation point on a sphere. Here $g = f$, so that

$$g''' + 2gg'' - (g')^2 + h = 0, \qquad (57)$$

and

$$h'' + 2\, Pr\, gh' = 0, \qquad (58)$$

subject to the boundary conditions (56).

Detailed numerical solutions of the above equations have been obtained for $Pr = 0{\cdot}72$ and $a = 0(\frac{1}{4})1$. The iterative procedure used to solve the non-linear boundary value problem will not be discussed as such methods have been adequately described by Fox [10]; the actual numerical integrations were carried out using Gill's modification of the Runge–Kutta procedure on an I.B.M. computer. Iterations were performed until there was no change in the eighth decimal of the unknown initial values $f''(0)$, $g''(0)$ and $h'(0)$; the numerical process appeared to be quite stable. In Table 1 the unknown characteristics of the equations, namely $f''(0)/a$, $g''(0)$, $h'(0)$, $f(\infty)/a$, $g(\infty)$ and $[g(\infty) + af(\infty)]$ are tabulated for $Pr = 0{\cdot}72$ and $a = 0(\frac{1}{4})1$. When $a = 0$ the notation f/a in Table 1 is used to denote $\underset{a \to 0}{\text{Limit}}\, f/a$.

4. APPROXIMATE SOLUTIONS OF THE BOUNDARY-LAYER EQUATIONS

It is found that the functions f, g and h vary most near $a = 0$. This feature, as will be later discussed, indicates how rapidly the free convection flow at a two dimensional stagnation point ($a = 0$) is affected by the presence of secondary flow ($a > 0$). Hence further information on flows for small a is desirable. Such information can be obtained on evaluation of series expansions for f, g and h valid for small a. However an approximate method of solution has been used which provides such information,

Table 1

a	0	$\frac{1}{4}$	$\frac{1}{2}$	$\frac{3}{4}$	1
$f''(0)/a$	1·08156	1·02881	0·929829	0·838737	0·764632
$g''(0)$	0·856045	0·845884	0·822382	0·794033	0·764632
$-h'(0)$	0·374105	0·383791	0·406247	0·433526	0·462221
$f(\infty)/a$	1·91331	1·70652	1·34349	1·04193	0·822524
$g(\infty)$	1·33255	1·26007	1·11030	0·956906	0·822524
$g(\infty) + af(\infty)$	1·33255	1·36673	1·44618	1·54299	1·64505
$-\dfrac{h(\infty)}{g(\infty) + af(\infty)}$	0·28074	0·28081	0·28091	0·28096	0·28098

and in fact provides complete information for the range $0 \leqslant \alpha \leqslant 1$.

For convenience, let

$$f = \alpha F, \quad g = G \quad \text{and} \quad h = H. \tag{59}$$

Equations (51) to (53) become:

$$\left.\begin{aligned} &F''' + (G + \alpha^2 F) F'' - \alpha^2 (F')^2 + H = 0, \\ &G''' + (G + \alpha^2 F) G'' - (G')^2 + H = 0, \\ &\text{and} \\ &H'' + Pr\,(\alpha^2 F + G)\, H' = 0, \end{aligned}\right\} \tag{60}$$

where

$$\left.\begin{aligned} &F(0) = F'(0) = G(0) = G'(0) = 0, \\ &H(0) = 1, \\ &F'(\infty) = G'(\infty) = H(\infty) = 0. \end{aligned}\right\} \tag{61}$$

Let the solutions of (60) and (61) be denoted by F_0, G_0, H_0, and F_1 G_1, H_1 when $\alpha = 0$ and 1

Approximations to F, G and H are now chosen by writing these as a linear combination of the exact numerical solutions for $\alpha = 0$ and 1. Thus

$$\left.\begin{aligned} F &= F_0 + A_1(\alpha)\,(F_1 - F_0), \\ G &= G_0 + A_2(\alpha)\,(G_1 - G_0), \\ H &= H_0 + A_3(\alpha)\,(H_1 - H_0). \end{aligned}\right\} \tag{62}$$

Here the unknown mixing parameters $A_i(\alpha)$ are such that $A_i(0) = 0$ and $A_i(1) = 1$ for $i = 1, 2$ and 3. Thus expressions (62) are correct at both limits, a desirable characteristic. The $A_i(\alpha)$ for $0 \leqslant \alpha \leqslant 1$ are evaluated using Pohlhausen's method (see reference [5b]).

Integrating each equation in (60) between the limits $\eta = 0$ and ∞ and using the boundary conditions (61) yields:

$$\left.\begin{aligned} &F''(0) - \int_0^\infty H\,d\eta + 2\alpha^2 \int_0^\infty (F')^2\,d\eta + \int_0^\infty G' F'\,d\eta = 0, \\ &G''(0) - \int_0^\infty H\,d\eta + 2 \int_0^\infty (G')^2\,d\eta + \alpha^2 \int_0^\infty G' F'\,d\eta = 0, \\ &H'(0) + P \int_0^\infty (\alpha^2 F' + G')\, H\,d\eta = 0. \end{aligned}\right\} \tag{63}$$

Physically the first two equations can be interpreted as the integral momentum equations for the components of velocity in the x_1 and x_2 directions; the third equation is the heat-balance integral of the thermal boundary layer. On substitution of expressions (62) in (63) three non-linear simultaneous algebraic equations are obtained for the $A_i(\alpha)$, $i = 1$, 2 and 3. As these equations are rather lengthy they will not be stated. However certain integrals occurring in these equations, such as $\int_0^\infty G_0' H_1\,d\eta$, cannot be expressed in terms of those obtained from (63) by letting $\alpha = 0$ or 1. Such integrals were evaluated by incorporating them as part of the Runge–Kutta integration of the system (60) and (61) for $\alpha = 0$ and 1, i.e. once the initial values $F_i''(0)$, $G_i''(0)$ and $H_i'(0)$ for $i = 1$ and 2 are known. The simultaneous equations were solved using the Choleski method together with a Gauss–Seidel iterative scheme for the treatment of the quadratic terms involving $A_i(\alpha)$, $A_2(\alpha)$ and $A_3(\alpha)$.

The mixing parameters $A_i(\alpha)$ and the corresponding results for $F''(0)$, $G''(0)$ and etc. are given in Table 2 for $\alpha = 0(0{\cdot}05)1{\cdot}0$ and $Pr = 0{\cdot}72$; these results are also given graphically in Fig. 1. When $\alpha = \frac{1}{4}, \frac{1}{2}$ and $\frac{3}{4}$ it is seen on comparing Tables 1 and 2 that the approximate results for the derivatives $F''(0)$, $G''(0)$ and $H'(0)$ are in error by less than $\frac{1}{2}$ per cent; the asymptotic values $F(\infty)$, $G(\infty)$, $[\alpha^2 F(\infty) + G(\infty)]$ are found to be in error by less than 3 per cent. Therefore the approximate method is sufficiently accurate for all practical purposes and has the advantage that detailed reliable information on the stagnation point flow on a general curved surface is relatively easy to obtain.

5. RESULTS AND DISCUSSION

Results of practical interest are the shear stress and heat transfer across the surface. On the basis of the boundary-layer approximations the shearing stress or skin friction across the surface has components:

$$\tau_1 = \mu \left(\frac{\partial v_1}{\partial x_3}\right)_{x_3=0} \text{and } \tau_2 = \mu \left(\frac{\partial v_2}{\partial x_3}\right)_{x_3=0}, \tag{64}$$

in the directions of x_1 and x_2 increasing. If R_2

Table 2

a	A_1	A_2	A_3	$F''(0)$	$G''(0)$	$-H'(0)$	$F(\infty)$	$G(\infty)$	$G(\infty)+a^2F(\infty)$
0·00	0·0000	0·0000	0·0000	1·0816	0·8560	0·3741	1·9133	1·3326	1·3326
0·05	0·0080	0·0052	0·0053	1·0790	0·8556	0·3745	1·9046	1·3299	1·3347
0·10	0·0313	0·0203	0·0209	1·0717	0·8542	0·3759	1·8792	1·3222	1·3410
0·15	0·0680	0·0449	0·0459	1·0600	0·8519	0·3782	1·8391	1·3097	1·3511
0·20	0·1157	0·0776	0·0795	1·0449	0·8489	0·3811	1·7871	1·2930	1·3645
0·25	0·1714	0·1175	0·1201	1·0272	0·8453	0·3847	1·7263	1·2726	1·3805
0·30	0·2325	0·1631	0·1665	1·0079	0·8411	0·3888	1·6597	1·2494	1·3988
0·35	0·2966	0·2133	0·2176	0·9876	0·8365	0·3933	1·5898	1·2237	1·4185
0·40	0·3618	0·2672	0·2722	0·9669	0·8316	0·3981	1·5186	1·1963	1·4393
0·45	0·4269	0·3239	0·3294	0·9463	0·8264	0·4031	1·4477	1·1674	1·4606
0·50	0·4907	0·3826	0·3886	0·9260	0·8211	0·4083	1·3780	1·1374	1·4820
0·55	0·5527	0·4427	0·4490	0·9064	0·8156	0·4137	1·3105	1·1068	1·5032
0·60	0·6124	0·5039	0·5104	0·8875	0·8100	0·4191	1·2453	1·0756	1·5239
0·65	0·6696	0·5657	0·5722	0·8694	0·8043	0·4245	1·1830	1·0440	1·5438
0·70	0·7242	0·6279	0·6341	0·8521	0·7986	0·4300	1·1234	1·0123	1·5628
0·75	0·7761	0·6903	0·6961	0·8356	0·7930	0·4354	1·0667	0·9805	1·5805
0·80	0·8256	0·7527	0·7578	0·8199	0·7872	0·4409	1·0127	0·9487	1·5956
0·85	0·8726	0·8149	0·8191	0·8050	0·7816	0·4463	0·9615	0·9169	1·6116
0·90	0·9172	0·8769	0·8800	0·7909	0·7759	0·4516	0·9128	0·8853	1·6247
0·95	0·9596	0·9386	0·9403	0·7774	0·7702	0·4570	0·8665	0·8538	1·6358
1·00	1·0000	1·0000	1·0000	0·7646	0·7646	0·4622	0·8225	0·8225	1·6450

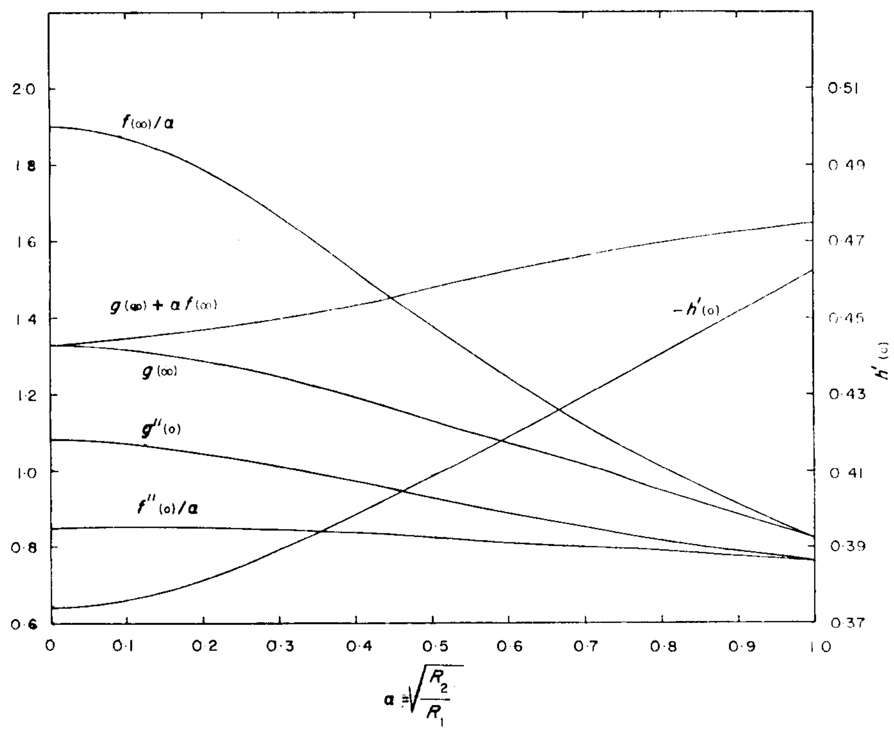

FIG. 1. Flow and heat-transfer characteristics for a stagnation point on a general curved surface.

is chosen as the representative length the heat transfer at the stagnation point may be expressed in terms of the local Nusselt number

$$Nu_0 = \frac{R_2}{(T_0 - T_\infty)} \left(\frac{\partial T}{\partial x_3}\right)_{x_3=0}. \quad (65)$$

Thus on using (43), (49) and (50) it follows that at the stagnation point

$$\tau_1 = \frac{\rho \nu^2}{R_2^2} \alpha^2 Gr^{1/4} \left(\frac{h_1 x_1}{R_2}\right) \frac{f''(0)}{\alpha},$$

$$\tau_2 = \frac{\rho \nu^2}{R_2^2} Gr^{1/4} \left(\frac{h_2 x_2}{R_2}\right) g''(0), \quad (66)$$

and

$$Nu_0 = Gr^{1/4} h'(0). \quad (67)$$

Values of $f''(0)/\alpha$, $g''(0)$ and $h'(0)$ are given in Tables 1 and 2 for $Pr = 0{\cdot}72$.

Velocity profiles

As α increases from zero the maximum velocity in the x_2-direction decreases slowly whilst there is a rapid increase in the maximum velocity in the x_1-direction, the two components of velocity becoming equal when $\alpha = 1$. Thus the secondary flow (or x_1-component of flow), which is due to curvature in the x_1-direction, has little influence on the main x_2-component of flow. However the occurrence of secondary flow when $\alpha > 0$ has an observable influence on the direction of the velocity vector in the boundary layer. For example the angle between the velocity vector at the surface and at the edge of the boundary layer is

$$\epsilon = \tan^{-1}\left[\left(\frac{h_1 x_1}{h_2 x_2}\right) \alpha \frac{f'(\infty)}{g'(\infty)}\right] - \tan^{-1}\left[\left(\frac{h_1 x_1}{h_2 x_2}\right) \frac{f'(0)}{g'(0)}\right]; \quad (68)$$

by L'Hopital's rule

$$\epsilon = \tan^{-1}\left[\left(\frac{h_1 x_1}{h_2 x_2}\right) \alpha \frac{f''(\infty)}{g''(\infty)}\right] - \tan^{-1}\left[\left(\frac{h_1 x_1}{h_2 x_2}\right) \frac{f''(0)}{g''(0)}\right], \quad (69)$$

and thus represents the angle between the resultant shear stress on S and at the edge of the boundary layer. Examination of the asymptotic form of the solution of the system of differential equations (51) to (53) leads to the result

$$\operatorname*{Limit}_{\eta \to \infty} \frac{f''(\eta)}{g''(\eta)} = \alpha,$$

and so

$$\epsilon = \tan^{-1}\left[\frac{\alpha^2 h_1 x_1}{h_2 x_2}\right] - \tan^{-1}\left[\frac{\alpha^2 h_1 x_1}{h_2 x_2}\left(\frac{f''(0)/\alpha}{g''(0)}\right)\right]. \quad (70)$$

From Table 1 the maximum changes in direction were evaluated to be 6·7°, 5·6°, 3·6°, 1·5° and 0° for $\alpha = \sqrt{(R_2/R_1)} = 0(\tfrac{1}{4})1$ respectively; the first four of these occurred at stations $\alpha^2 (h_1 x_1/h_2 x_2) = 0{\cdot}89, 0{\cdot}91, 0{\cdot}94$ and $0{\cdot}97$ respectively.

Heat transfer

As secondary flow increases with increasing α there is an increase in the inflow velocity $v_3 = -\nu/R_2\,[\alpha f(\infty) + g(\infty)]$ at the edge of the boundary layer (see Fig. 1). An increase in inflow appears to produce a slight decrease in both the thermal and fluid boundary-layer thicknesses, together with an increase in the local Nusselt number $Nu_0 = Gr^{1/4}h'(0)$ (see Fig. 1). Actually maximum heat transfer occurs when $\alpha = 1$, i.e. at the lower stagnation point on a sphere. Again from Table 1 it is seen that the modulus of the ratio

$$\left(\frac{\text{Local Nusselt number at the stagnation point}}{\text{Inflow velocity component at the edge of the boundary layer}}\right) = 0{\cdot}2809 \frac{R_2}{\nu} Gr^{1/4} \quad (71)$$

approximately, when $P = 0{\cdot}72$ and $0 \leqslant \alpha \leqslant 1$. Thus once a representative length R_2 has been chosen the above ratio is independent of R_1, as it is seen to be nearly independent of the curvature ratio

$$\alpha = \sqrt{\left(\frac{R_2}{R_1}\right)}.$$

From an experimental viewpoint (71) might be exploited as Nu_0 could be evaluated by measuring the inflow velocity component for R_2 and

$(T_0 - T_\infty)$ fixed, and for various values of R_1. A suitable body for experimentation might be an anchor ring maintained at constant temperature, and whose axis of revolution is horizontal.

Finally as an illustration of the above theory consider the geometrical information required to discuss the local stagnation point free convection flow on an ellipsoid of revolution whose equation is

$$\frac{x^2}{a^2} + \frac{y^2}{a^2} + \frac{z^2}{b^2} = 1, \qquad (72)$$

and whose axis of revolution is horizontal. If $T_s > T_\infty$ the lower stagnation point is situated at $(0, -a, 0)$. Orthogonal parametric co-ordinates are chosen such that (72) is replaced by

$$\mathbf{r} = a \cos x_1 \sin x_2 \,\mathbf{i} - a \cos x_1 \cos x_2 \,\mathbf{j} - b \sin x_1 \,\mathbf{k}, \qquad (73)$$

where $\mathbf{i}$, $\mathbf{j}$ and $\mathbf{k}$ are unit vectors in the directions of the Cartesian co-ordinates x, y and z respectively; $x_1 = x_2 = 0$ corresponds to the lower stagnation point. The evaluation of (20) yields:

$$\left.\begin{aligned} E &= a^2 \sin^2 x_1 + b^2 \cos^2 x_1, \\ F &= 0 \\ G &= a^2 \cos^2 x_1, \\ (EG\ F^2)^{1/2} L &= a^2 b \cos x_1, \\ (EG - F^2)^{1/2} M &= 0, \\ (EG - F^2)^{1/2} N &= a^2 b \cos^3 x_1. \end{aligned}\right\} \qquad (74)$$

As F and M both vanish the chosen parametric lines $x_1 = \text{const.}$ and $x_2 = \text{const.}$ are in fact the lines of curvature on the surface; at $x_1 = x_2 = 0$, $LN > M^2$ and so the stagnation point is an elliptic point of the surface. At the stagnation point

$$E = h_1^2 = b^2, \quad F = 0, \quad G = h_2^2 = a^2,$$
$$L = a, \quad M = 0, \quad N = a \qquad (75)$$

and thus

$$R_2 = a \quad \text{and} \quad R_1 = \frac{b^2}{a}, \qquad (76)$$

giving

$$\alpha = \sqrt{\left(\frac{R_2}{R_1}\right)} = \frac{b}{a}; \qquad (77)$$

$\alpha = 0$ and 1 correspond to a uniform horizontal cylinder and a sphere respectively.

REFERENCES

1. A. J. Ede, Natural convection on free vertical surfaces, M.E.R.L. Report Heat 141. East Kilbride, Glasgow: Mechanical Engineering Laboratory (1956).
2. H. J. Merk and J. A. Prins, Thermal convection in laminar boundary layers I, II, *Appl. Sci Res.* **A4**, 11–24; 195–206 (1954).
3. W. H. Braun, S. Ostrach and J. E. Heighway, Free convection similarity flows about two-dimensional and axisymmetric bodies with closed lower ends, *Int. J. Heat Mass Transfer* **2**, 121–135 (1961).
4. R. G. Hering and R. J. Grosh, Laminar free convection from a non-isothermal cone, *Int. J. Heat Mass Transfer* **5**, 1059–1068 (1962).
5. L. Rosenhead (Ed.), *Laminar Boundary Layers*, (a) chapter VIII, (b) chapter VI. University Press, Oxford (1963).
6. L. Howarth, The boundary layer in three-dimensional flow—Part II. The flow near a stagnation point, *Phil. Mag.* Series 7, **42**, 1433–1440 (1951).
7. C. E. Weatherburn, *Differential Geometry of Three Dimensions*, Vol. I. University Press, Cambridge (1927).
8. R. Hermann, Heat transfer by free convection from horizontal cylinders in diatomic gases. *NACA TM* 1366 (1954).
9. M. M. Chen, An analytical study of laminar film condensation: part 2—single and multiple horizontal tubes. *J. Heat Transfer* **C83**, 55–60 (1961).
10. L. Fox (Ed.), *Numerical Solution of Ordinary and Partial Differential Equations*, Chapter 5. Pergamon Press, Oxford (1962).

Résumé—Cet article a trait à quelques aspects de la couche limite laminaire tridimensionnelle avec convection libre près du point d'arrêt sur une surface courbe générale isotherme, qui est maintenue à une température au-dessus de la température ambiante du fluide. Ainsi, le point d'arrêt est défini comme le point (elliptique) le plus bas sur la surface et tel que le plan tangent en ce point soit horizontal. Les équations de la couche limite sont formulées et on montre que l'écoulement au point d'arrêt dépend du rapport des deux rayons de courbure principaux en ce point, du nombre de Prandtl et du nombre de Grashof. Ces équations sont résolues numériquement pour un nombre de Prandtl de 0,72 et pour différentes valeurs du rapport des deux rayons de courbure principaux.

Pour le point d'arrêt, il y a deux cas limites, c'est-à-dire l'écoulement à la ligne d'arrêt la plus basse sur un cylindre horizontal uniforme et celui au point d'arrêt le plus bas sur une sphère. Les solutions numériques pour la sphère et le cylindre sont alors utilisées pour développer une méthode approchée de solution pour le point d'arrêt sur une surface courbe générale; on a obtenu un bon accord avec les solutions numériques exactes.

Zusammenfassung—Die Arbeit behandelt einige Gesichtspunkte der dreidimensionalen Grenzschicht bei laminarer freier Konvektion nahe dem Staupunkt an einer allgemein gekrümmten, isothermen Oberfläche, deren Temperatur über jener der Umgebung gehalten wird. Dabei ist der Staupunkt als der tiefste (elliptische) Punkt der Oberfläche definiert, so dass die Tangentenebene an diesem Punkt horizontal ist. Grenzschichtgleichungen werden aufgestellt und es wird gezeigt, dass die Strömung am Staupunkt, vom Verhältnis der zwei Hauptkrümmungsradien an diesem Punkt, der Prandtl-Zahl und der Grashof-Zahl abhängt. Diese Gleichungen werden numerisch gelöst für die Prandtl-Zahl 0,72 und für verschiedene Verhältniswerte der beiden Hauptkrümmungsradien.

Für die Staupunktsströmung existieren zwei Grenzfälle-nämlich die Strömung an der unteren Staulinie eines gleichförmigen, waagerechten Zylinders und die Strömung am unteren Staupunkt einer Kugel. Die numerischen Lösungen für Kugel und Zylinder können dazu dienen, eine angenäherte Lösungsmethode für den Staupunkt einer allgemein gekrümmten Oberfläche zu entwickeln; gute Übereinstimmung mit den genauen numerischen Lösungen wird erreicht.

Аннотация—Данная статья рассматривает некоторые аспекты трехмерного ламинарного пограничного слоя при свободной конвекции вблизи критической точки на произвольной криволинейной изотермической поверхности, которая поддерживается при температуре, выше температуры окужающей жидкости. Таким образом, критическая точка определяется как самая нижняя (эллиптическая) точка на поверхности так, что касательная плоскость в этой точке является горизонтальной. Формулируются уравнения пограничного слоя. Показано, что поток в критической точке зависит от отношения двух основных радиусов кривизны в этой точке, числа Прандтля и числа Грасгофа. Эти уравнения решаются численно для $Pr = 0{,}72$ и для различных значений отношения двух основных радиусов кривизны.

Для потока в критической точке существует два предельных случая, а именно: поток в нижней критической точке на однородном горизонтальном цилиндре и поток в нижней критической точке на шаре. Затем, численные решения для шара и цилиндра используются для построения приближенного метода решения критической точки на произвольной криволинейной поверхности. Получено хорошее согласование с точными численными решениями.